Efficient Drone-Based Rare Plant Monitoring Using a Species Distribution Model and AI-Based Object Detection

William Reckling [1,2,*], **Helena Mitasova** [1,2], **Karl Wegmann** [1,2], **Gary Kauffman** [3] **and Rebekah Reid** [4]

1   Center for Geospatial Analytics, North Carolina State University, Raleigh, NC 27695, USA; hmitaso@ncsu.edu (H.M.); karl_wegmann@ncsu.edu (K.W.)
2   Marine, Earth and Atmospheric Sciences, North Carolina State University, Raleigh, NC 27695, USA
3   US Forest Service, Asheville, NC 28801, USA; gary.kauffman@usda.gov
4   US Fish and Wildlife Service, Asheville, NC 28801, USA; rebekah_reid@fws.gov
*   Correspondence: wjreckli@ncsu.edu

Abstract: Monitoring rare plant species is used to confirm presence, assess health, and verify population trends. Unmanned aerial systems (UAS) are ideal tools for monitoring rare plants because they can efficiently collect data without impacting the plant or endangering personnel. However, UAS flight planning can be subjective, resulting in ineffective use of flight time and overcollection of imagery. This study used a Maxent machine-learning predictive model to create targeted flight areas to monitor *Geum radiatum*, an endangered plant endemic to the Blue Ridge Mountains in North Carolina. The Maxent model was developed with ten environmental layers as predictors and known plant locations as training data. UAS flight areas were derived from the resulting probability raster as isolines delineated from a probability threshold based on flight parameters. Visual analysis of UAS imagery verified the locations of 33 known plants and discovered four previously undocumented occurrences. Semi-automated detection of plant species was explored using a neural network object detector. Although the approach was successful in detecting plants in on-ground images, no plants were identified in the UAS aerial imagery, indicating that further improvements are needed in both data acquisition and computer vision techniques. Despite this limitation, the presented research provides a data-driven approach to plan targeted UAS flight areas from predictive modeling, improving UAS data collection for rare plant monitoring.

Keywords: UAS; flight planning; orthomosaic; species distribution modeling; endangered species; *Geum Radiatum*; Blue Ridge Mountains; object detection; machine learning; cliff mapping

1. Introduction

Accurately monitoring rare plant populations is critical to identifying threats to occurrences and establishing long-term population trends. Monitoring is the repeated process of collecting and analyzing data about a species to evaluate progress towards a management objective [1,2]. In the United States, monitoring is mandated by the U.S. Congress, the federal Bureau of Land Management, and the individual States. Federal regulations such as The Endangered Species Act, National Environmental Policy Act, and Federal Land Policy Act outline the steps to protect and recover endangered species. For example, in North Carolina, the State Endangered Species Act directs officials to bring populations of native species in balance with their habitat and then maintain them to the point at which the measures are no longer necessary. The methods include resource management activities such as research, census, habitat protection, and species restoration to unoccupied parts of the historic range [3].

To fulfill the monitoring mandates, conservation biologists need to identify plant populations and conduct long-term demographic studies as efficiently as possible. These studies rely on field observations from personnel with varying skill levels. As a result,

differences in detection among observers may occur, and population sizes might be incomplete or underestimated. A miscount of plants in a census can lead to biased population health and extent estimates [1].

Rare plants are often located in hard-to-access areas that may pose challenges for conducting detailed surveys (e.g., cliffs). Traditional ground-based monitoring methods can be resource-intensive and dangerous when performed in overgrown, rough, or steep terrain [4]. Unmanned aerial systems (UAS) provide powerful tools for monitoring rare plants with little inherent risk to personnel or the species being monitored [5]. It has been demonstrated that UAS can cost-effectively collect detailed data in rugged alpine and cliff environments [6–10]. UAS have been used for various conservation purposes, including law enforcement, disaster response, environmental monitoring, and management [11]. High-resolution photographs and 3D models generated from UAS imagery have been used to identify plant locations, measure plant distribution, and gather data on their habitat [4].

However, planning UAS flight paths is somewhat subjective and can result in inefficient usage of limited flight time or overcollection of data [12]. There are examples of UAS flight preplanning to search for poachers [12] and to optimize imagery/data collection for tree structure monitoring [13]. Additionally, probability mapping has been used to plan UAS flight paths for search and rescue [14–16] and even as a method to direct autonomous underwater vehicles [17].

Although species distribution modeling and UAS plant monitoring have been individually used for species conservation, we present a method that combines them to improve the efficiency of UAS-based plant monitoring and facilitate the potential discovery of unknown plant locations. We first outline the general workflow for the proposed approach and then demonstrate its implementation and application for monitoring the rare plant species, *Geum radiatum*, to a site in the Blue Ridge Mountains in North Carolina. Next, we describe the machine-learning predictive model used to create UAS flight areas with a high probability of these species' locations and evaluate which predictors are significant variables in determining these locations. Finally, we collect and analyze the UAS data in one of the high probability areas and assess whether the collected UAS imagery is of sufficient detail to identify rare plants at the test location. We also discuss the potential for using object detection and feature extraction to automate the monitoring process further.

2. Materials and Methods

To target UAS monitoring of rare plants in challenging-to-inaccessible locations and acquire UAS data with a high probability of finding new plant locations, we propose a general approach/workflow that combines machine learning with UAS flight planning designed explicitly for a studied plant (Figure 1). We also discuss the potential for using object detection to further automate the monitoring process. Given the plant species and a general region where it should be monitored, environmental data layers were identified and derived, which characterize the ecosystem favorable for a plant at a study site. Using these layers and known plant locations, a predictive model was developed to map plant location probabilities. Species distribution is modeled with a maximum entropy machine-learning method implemented in Maxent [18]. A probability threshold is selected to delineate the flight area for targeted monitoring based on flight parameters (height, overlap, ground sample distance, pattern) and UAS endurance (battery and weather). Topographic and environmental conditions at the selected areas are analyzed, and the flight pattern design is optimized for the specific location. If the area is in complex or steep topography, daytime shadow evolution is computed to identify the time of day to fly with minimum shadowing effect. The acquired data are then processed, and an orthomosaic, point cloud, and digital surface model (DSM) are derived. These provide input for identifying target plant locations using visual analysis or semi-automated approaches depending on species properties and the mapped area environment.
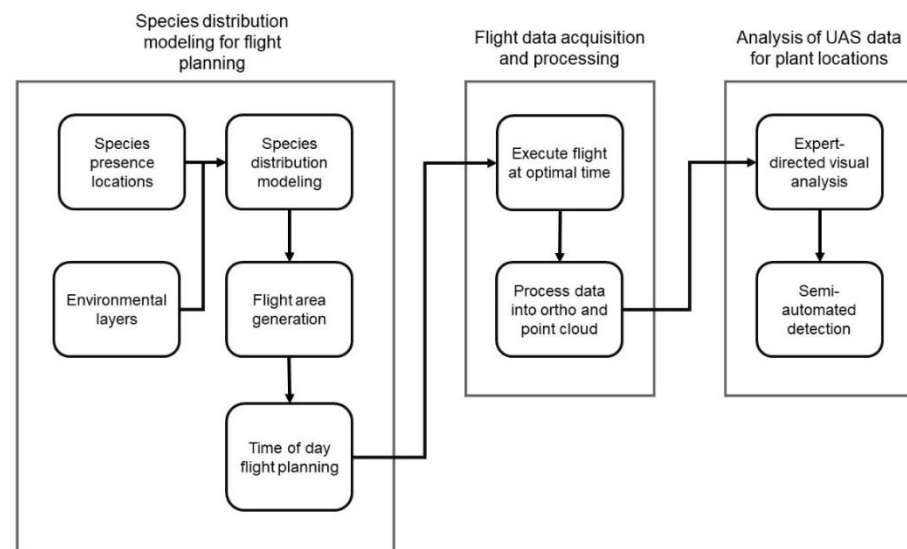
Figure 1. Diagram of targeted UAS monitoring workflow.

The Blue Ridge Mountains in North Carolina and *Geum radiatum, a* rare plant species (Figure 2), were selected to develop and test the proposed methodology and evaluate the feasibility of the proposed approach. The high mountains and cliff faces provide a challenging environment to conduct plant monitoring.

Figure 2. Blooming *Geum radiatum* plant (kidney-shaped leaves with yellow flowers) photographed on a narrow, rocky ledge at Roan Mountain.

2.1. Study Species

Geum radiatum, commonly known as Spreading Avens, is a federally listed endangered plant species [19] native to the Blue Ridge Mountains of North Carolina and Tennessee [20] (Figure 2). *Geum radiatum* is found on rocky outcrops and bluffs at elevations ranging from 1400 to 1911 m [20]. It is a rhizomatous perennial herb in the rose family with 7–15 cm wide leaves, up to 2.5 cm bright yellow flowers [20–22], and a patch of rosettes covers around 1.7 m^2 [23]. This species requires direct sunlight for part of the day with a west/southwest to north/northeast facing aspect [19]. *Geum radiatum* grows in shallow, acidic soils that range from moderately poorly drained to excessively drained. The specimens identified in this study on the cliff face exist in the

shallowest of excessively drained soil conditions; however, the flow of moisture along rock crack surfaces likely aids in bringing water to the plants during dry intervals. [20]. The soils remain damp from high-elevation fog which also prevents solar evaporation [19]. During the last glacial maximum, *Geum radiatum* was part of a more widespread alpine community. *Geum radiatum* likely experienced a shrinking habitat as the climate warmed and vegetation zones moved northward [24,25]. Niche habitats offer protection for rare plants during climatic fluctuations, and this species has been able to survive on the cool cliffs of the Blue Ridge Mountains [26,27]. Suitable habitats for *Geum radiatum* are expected to retract further because of future climate change [26]. Recreational hikers, climbers, and development pose threats to the species. Efforts to barricade sites and educate the public have been implemented as protection measures [19]. There are 15 known *Geum radiatum* locations, and 11 occur on publicly owned lands [28]. Populations may be undercounted because of inconsistent monitoring methods among personnel [28], and access to the plants often requires skilled rock climbers and equipment [20]. The species was federally listed as endangered on 5 April 1990 [19].

The 1993 recovery plan for *Geum radiatum* outlines five actions needed to recover the species, two of which apply to this study; "Survey suitable habitat for additional populations" and "monitor and protect existing populations" [19]. The species recovery plan further describes a systematic search for additional populations that should begin with an analysis of aerial photos and topographic maps to identify habitat and "develop a priority list of sites to search" [19] (p. 5). Additionally, the document recommends long-term demographic studies where the plots are visited annually and "the locations of individual plants should be mapped or photographed" [19] (p. 21). A demographic study conducted annually in July between 2003 to the present involves rappelling to sites along cliffs, marking plant locations, and recording descriptors. Plant locations were recorded in horizontal coordinates (e.g., UTM easting, northing) and written descriptions referenced to the cliffs they were found growing on [29]. The emergence of UAS technologies and machine-learning workflows provides technological solutions and opportunities to improve the documentation and monitoring of known occurrences and the prospect for additional cliff-born enclaves of *Geum radiatum*.

2.2. Species Distribution Modeling for Flight Planning

To target the UAS mapping at locations with the highest probability of finding a target plant species, a maximum entropy machine-learning algorithm was used for modeling species geographic distributions [18] that is available in Maxent 3.41 [30] under an open-source MIT license [31]. Species distribution modeling (SDM) is used in rare plant management applications, highlighting areas for targeted searches or restoration efforts [32]. Maxent has been cited as the most widely used SDM method [31,33,34]. It has performed well against other SDM methods, including models with presence/absence data (regression, random tree) [35]. Maxent works well with limited training data and can be run with as few as 5 point locations. Additionally, the regularization method in the model lessens the need to remove or preprocess correlated environmental variables [36,37]. Maxent requires two sets of input data: species presence locations and environmental layers [31]. Species presence locations are training data for the model given by geographic coordinates of known species occurrences. Environmental layers are predictors for the model represented as raster grids of environmental variables [18,38].

2.2.1. Species Presence Locations

The North Carolina Natural Heritage Program (NHP) maintains an inventory of rare plants, animals, and communities in North Carolina. Specific occurrences of these groups are known as elements and are stored as georeferenced polygons in a natural heritage element occurrences shapefile [39] which is updated on a quarterly basis. QGIS 2.18.7 [40] was used to extract *Geum radiatum* polygons from the inventory resulting in 44 polygons ranging in sizes from 40 m^2 to 2.7 km^2 and a median size of 3278 m^2. The extracted *Geum radiatum* polygons were converted to centroids within polygons to approximate plant

locations for model training and then reprojected to the geographic WGS84 coordinates required by Maxent (Figure 3).
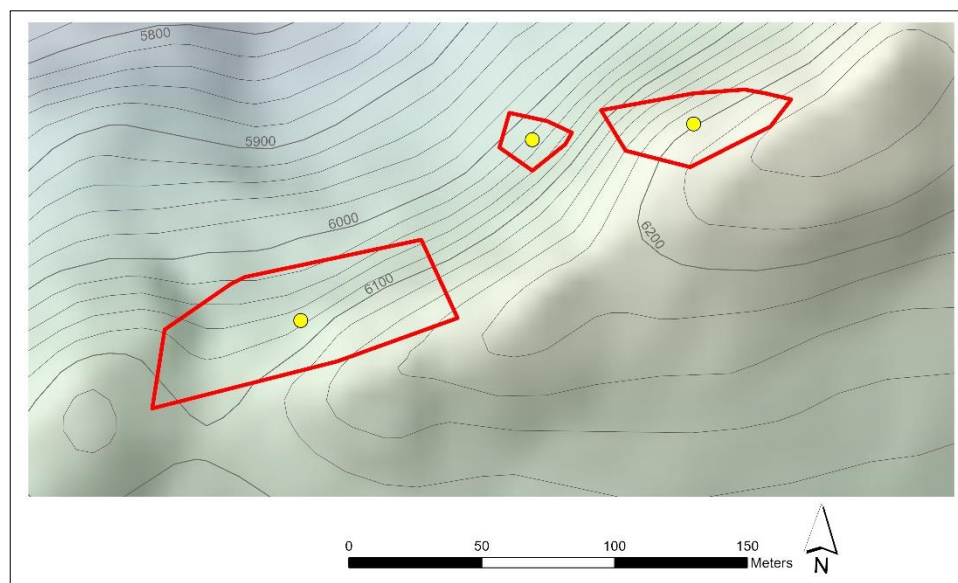
Figure 3. Example *Geum radiatum* species presence locations from the N.C. Natural Heritage Program database converted from polygons to centroids and overlain on a shaded relief. Specific location information is purposefully not included.

2.2.2. Environmental Layers

Environmental layers, also referred to as covariates or predictors, are the independent variables used in the SDM [36]. Ten variables were selected based on relevance to habitat preferences described in a plant survey for *Geum radiatum* conducted by Massey et al. (1980) (Table 1) and availability of data at adequate resolution. The data were acquired from public repositories, processed into a common raster representation required by Maxent, and clipped to the Blue Ridge ecoregion (Figure 4).

Table 1. *Geum radiatum* habitat preferences.

Variable	Attributes
Climate	Cool, cloudy, windy
Soil	Clay loam, loam, sandy loam, hummus soils
Geology	Rock substrates composed of muscovite and quartz schist or phyllite, biotite, quartz diorite, granitoid gneiss, and garnet rich mica
Hydrology	Moderate poorly drained to excessively drained
Topography	Cliff faces and ledges, outcropping and scattered boulders, or exposed mountain peaks with 10% to 90% exposure. Rounded mountain tops, bluff/cliff faces open to partly sheltered. Surface cracks and crevices serve for placement of grass mounds and moss, which influence the surface features. 0–90-degree slopes on W, WNW, NW, NNW, and NNE exposures
Physiography	Elevation of 1400 to 2100 m
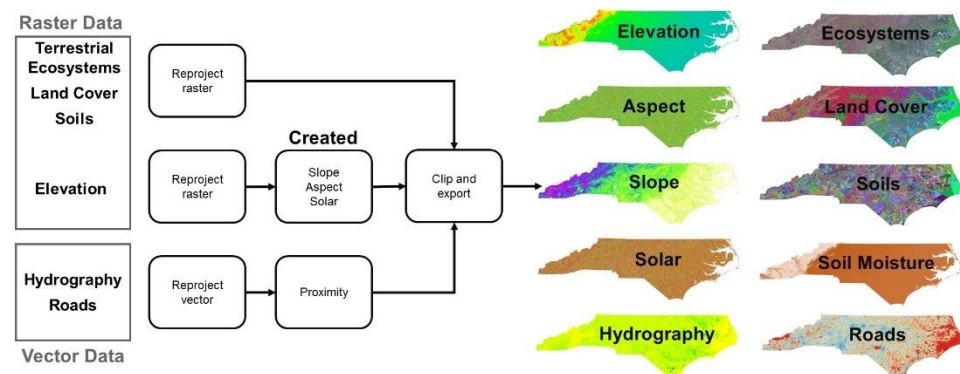
Figure 4. Environmental layer processing steps for raster and vector data. Input raster layers were reprojected and resampled to a common resolution of 0.22 arcsec (equivalent to approximately 6 m resolution of the original DEM) in the WGS84 coordinate reference system. Proximity operation was used to create a raster grid from the input vector layers at the same resolution.

Elevation [41] was available as a digital elevation model (DEM) raster layer at 20 ft (~6 m) resolution in NAD 1983 State Plane EPSG:2264 coordinate system. It was reprojected to 0.22 arcsec resolution (equivalent to its original resolution of ~6 m) in WGS84 EPSG:4326 coordinate system using the warp function in QGIS (Figure 4). *Slope* and *aspect* raster layers were then derived from this DEM. A *solar radiation* raster representing the maximum daily total radiation was computed from the DEM, aspect, and slope raster layers [42]. The day of summer solstice was selected to represent maximum daily total radiation under clear sky conditions for the longest day of the plant growing season.

Land cover [43], GAP/LANDFIRE national *terrestrial ecosystems* [44], and *soil type and moisture* [45] were available as raster layers at 30 m, 30 m, and 10 m resolutions respectively in NAD 1983 UTM Zone 17N EPSG:26917, NAD83 Conus Albers EPSG:5070, and USA Contiguous Albers Equal Area Conic USGS WKID:102039 coordinate system(s). To match the elevation data resolution and coordinate system, these layers were resampled and reprojected to a common resolution of 0.22 arcsec in WGS84 EPSG:4326 coordinate system using the warp function in QGIS (Figure 4). The nearest-neighbor method was used to resample these discrete data to preserve the values and grain of the original data and to avoid introducing new, potentially artificial values. National Hydrography Dataset line and polygon features [46], and North Carolina road line features [47] were first reprojected from the NC State Plane coordinate system EPSG:2264 to WGS84 EPSG:4326 and then *proximity to hydrography* and *proximity to roads* raster layers were derived at 0.22 arcsec resolution (equivalent to approximately 6 m).

All derived raster layers were generated in GRASS GIS 7.4.0 [48]. Each of the ten environmental layers was then masked to the Blue Ridge ecoregion polygon boundaries [49] (Figure 5) and exported in asci format required by Maxent with the common coordinate reference system and identical spatial extents.
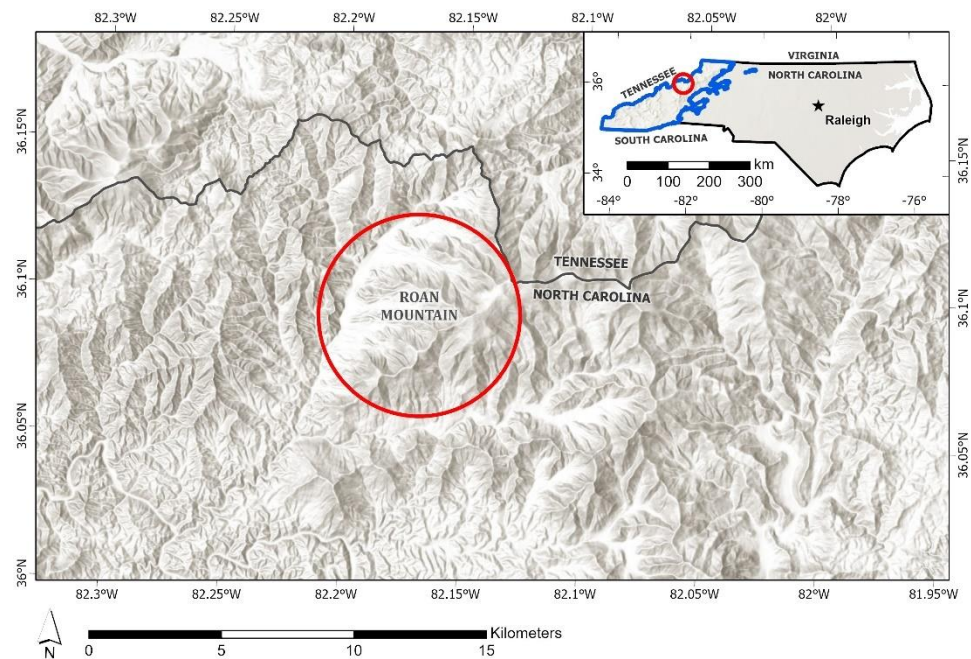
Figure 5. Study site (red circle) located on Roan Mountain, situated within the Blue Ridge ecoregion (blue line), in westernmost North Carolina, USA. (top-right).

2.2.3. Modeling Species Distribution

The Maxent predictive model was developed with the ten environmental layers as predictors, and the species presence location points approximated by polygon centroids (*n* = 44) as training data. The model was run for the Blue Ridge ecoregion with 5-fold cross-validation, where 20% of the training data were withheld for each of the five model runs. Default Maxent parameters were used, but the iterations value increased to 5000, which allows the model sufficient iterations for the optimization algorithm to converge [50,51]. The resulting raster map shows the predicted probability that conditions are suitable for the modeled species. The summary of model performance includes a statistical analysis of the test omission rate and the receiver operating characteristic (ROC) curve [52]. It also provides an analysis of variable contributions that show which predictors influence the model the most and response curves that highlight the most important attributes within each predictor [52].

The UAS flight areas were then derived from the probability raster as isolines with a selected probability threshold, in our case set to 95%.

2.2.4. Flight Path Generation

A 95% probability area located on Roan Mountain (36.106292° N, −82.111041° W) was selected to test the proposed UAS-based monitoring methodology. This area has a well-documented *Geum radiatum* plant community, a launch area free from overhead obstruction, and relatively easy access from a 1.9 km hiking trail. Roan Mountain is situated along the border of North Carolina and Tennessee within the Pisgah (NC) and Cherokee (TN) National Forests (Figure 5). One of the five peaks comprising Roan Mountain has an elevation of 1910 m [53] and is one of the highest points in North Carolina [54]. The high elevation creates a unique ecoregion that contains 47 plant species monitored by the North Carolina Natural Heritage Program. Of these plant species, four are listed as federal species of concern, and four are listed as endangered or threatened [39].

The 95% probability polygon covering the study site was imported into the DroneDeploy flight planning web application [55] (Figure 6). The flight was programmed to be flown in a crosshatch pattern with the auto flight mode feature. This flight mode ensures close to nadir views by minimizing banking turns and through use of the UAS gimbal. Although the DroneDeploy software defaults to a front and sidelap of 50% in crosshatch

auto flight mode to limit data size, frontal and side image overlap increased to 65% to improve feature matching [56].

Figure 6. Targeted flight area polygon uploaded into DroneDeploy flight planning web application. White points are the 95% probability polygon vertices, and the green dotted line is the crosshatch flight path for the UAS. This flight area polygon is within the study site shown in Figure 5. Due to restrictions on sharing rare plant information, the authors were asked to avoid showing exact details/locations.

2.2.5. Time of Day Flight Planning

Previous experience with UAS mapping in mountainous regions highlights the difficulty of capturing cliff imagery without shadows [6,57]. Therefore, a shadow model was created for the study area to determine the best time for UAS imagery capture to minimize imaging areas in the shade. A GRASS GIS hourly solar insolation model was calculated using an available 1 m resolution LiDAR derived DEM [58] for one-hour increments. The output indicated a window between 12:00 p.m. and 2:00 p.m. to have the least shadow along the cliff face (Figure 7).
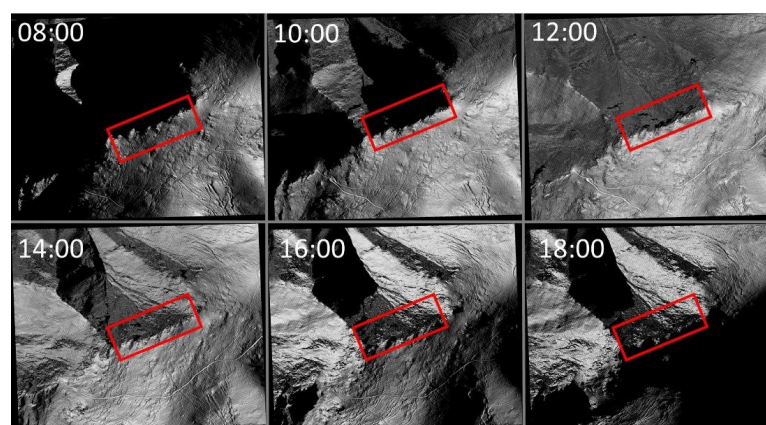
Figure 7. Solar models depicting cast shadows at the Roan Mountain study site (red box). Black shading represents modeled shade areas.

2.3. Flight Data Acquisition and Processing

Because the Roan Mountain flight area spans two National Forests and is near the Appalachian Trail (a no-fly zone), UAS flight authorization was coordinated with the U.S. Forest Service, U.S. Fish and Wildlife Service, and the National Park Service. Three UAS flights were executed at the Roan Mountain study site at 1:30 p.m. on 25 July 2019, with a DJI Phantom 4 Advanced quadcopter with a 24 mm, 20-megapixel RGB sensor. The UAS sensor was set to 90 degrees nadir camera angle, manual focus set to infinity, and f2.8 aperture. The first two flights were flown at 30 m above the ground altitude at takeoff. As a precautionary measure, the second flight was flown with the same parameters except for changes to the flight pattern from a crosshatch to a linear path and an increase in overlap to 75%. The linear flight path allowed for shorter flight duration and was only collected as backup data. These flights were autonomously flown and controlled with the Android DroneDeploy Flight App [59] previously configured with the targeted flight area. The third flight was flown manually to collect photographs at a 40-degree oblique angle with the DJI Go app [6] to collect more detailed imagery of the vertical cliff face [60]. The live video feed and distance measurements in the DJI app were used to estimate overlap as the UAS moved along and down the cliff face.

The high-resolution RGB aerial photography from the first and third flights was processed in Agisoft Metashape 1.6.3 [61]. Imagery collected from the first flight was sufficient, and the redundant second flight data set was unnecessary. The imagery was processed with high quality and accuracy settings with mild depth filtering to eliminate noise in the point cloud [62]. A 3D mesh and interpolated digital surface model (DSM) were created from the point cloud. An orthomosaic was generated by rectifying the images to the DSM. An orthomosaic, digital surface model (DSM), and point cloud were exported for analysis in GIS software. Ground control and checkpoints were not collected or used in the imagery processing; the steep terrain and heavy canopy made target placement and survey unattainable.

2.4. Analysis of UAS Data for Plant Locations

The UAS aerial imagery and orthomosaics were visually analyzed to identify the plant locations, and semi-automated detection of target plant species was explored using computer vision.

2.4.1. Expert-Directed Visual Analysis

UAS orthomosaics have been successfully used to identify plant locations and characteristics [4]. However, in a heavily forested area, detail from the source images can be lost in the process as the orthophoto rectification process may omit canopy gaps and smooth tree crowns [63]. Therefore, rather than inspecting the orthomosaic or individual orthophotos, each uncorrected UAS aerial photo was visually analyzed for *Geum radiatum* leaves/flowers. To help spatially locate the position of each photo, points representing the center of the images in QGIS were created with the ImportPhotos plugin [64] (Figure 8). The points were displayed over the orthomosaic, which facilitated the detection of plants in their correct geographic locations. The orthomosaic was then used for digitizing polygon outlines of the known and previously unknown *Geum radiatum* plant patches in a GIS.
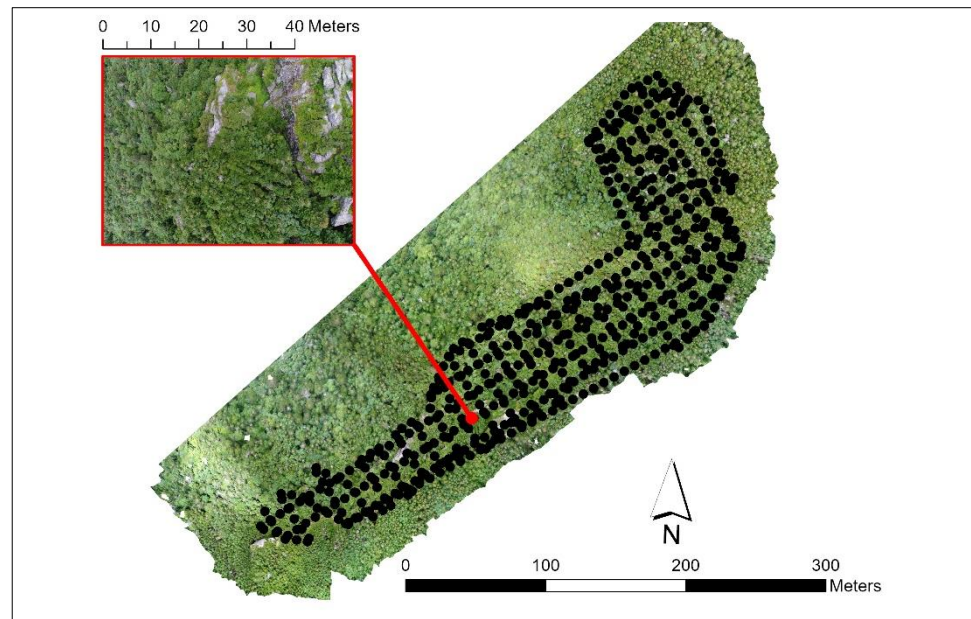
Figure 8. Orthomosaic with the point locations of each UAS aerial photograph. A single aerial photo containing a *Geum radiatum* plant is shown with its associated point.

2.4.2. Semi-Automated Detection with Computer Vision

Computer vision methods have been successfully implemented to identify, count and capture the morphological features of plants [65]. An approach to semi-automated identification of plants was explored with a YOLO (You Only Look Once) neural network object detector. The Visual Object Tagging Tool [66] was used to label *Geum radiatum* plants in 73 photos downloaded from an internet search and taken by the authors (Figure 9). The labels were used to train a model using the darknet neural network framework [67] for generating custom models. This methodology was selected because of its successful implementations in the agricultural industry and with UAS datasets [68,69]. YOLOv3 [70] was used to explore the possibility of detecting the *Geum radiatum* plants on the UAS aerial imagery.
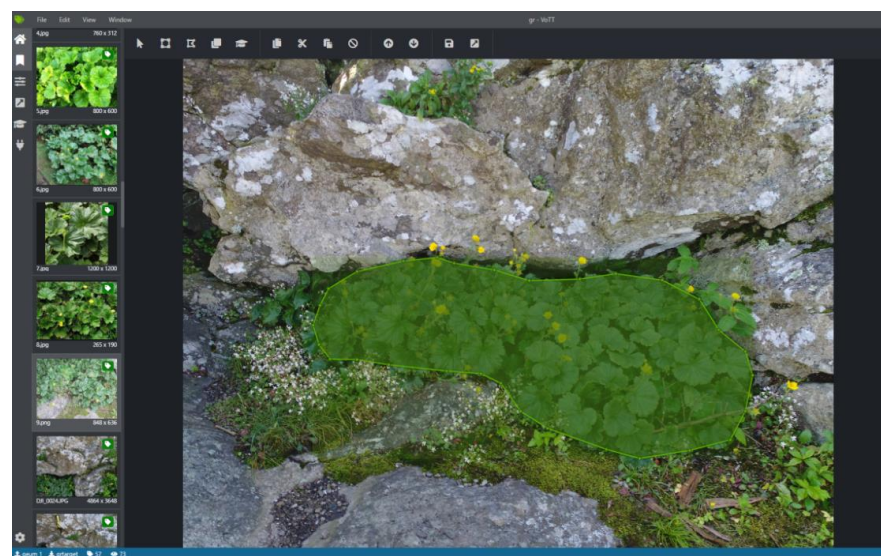
Figure 9. *Geum radiatum* leaves and flowers are enclosed (labeled) with the green polygon in the Visual Object Tagging Tool software.

3. Results

3.1. Species Distribution Modeling

Maxent modeling resulted in a raster map with a probability of *Geum radiatum* presence value for each cell for the entire Blue Ridge region (Figure 10). The replicate Maxent algorithms converged after 500 to 720 iterations. The statistical analysis from the *Geum radiatum* Maxent run averaged over five replicates shows an excellent match between the predicted omission rate and test omission rate on test samples (see Appendix A, Figure A1). The receiver operating curve (ROC) evaluation shows predictions regarding the area under the curve (AUC). AUC measures the probability that a random presence site was ranked higher than a random absence site. The AUC for *Geum radiatum* was 0.997, and the standard deviation was 0.001, which demonstrated a high accuracy [51] (see Appendix A, Figure A2).
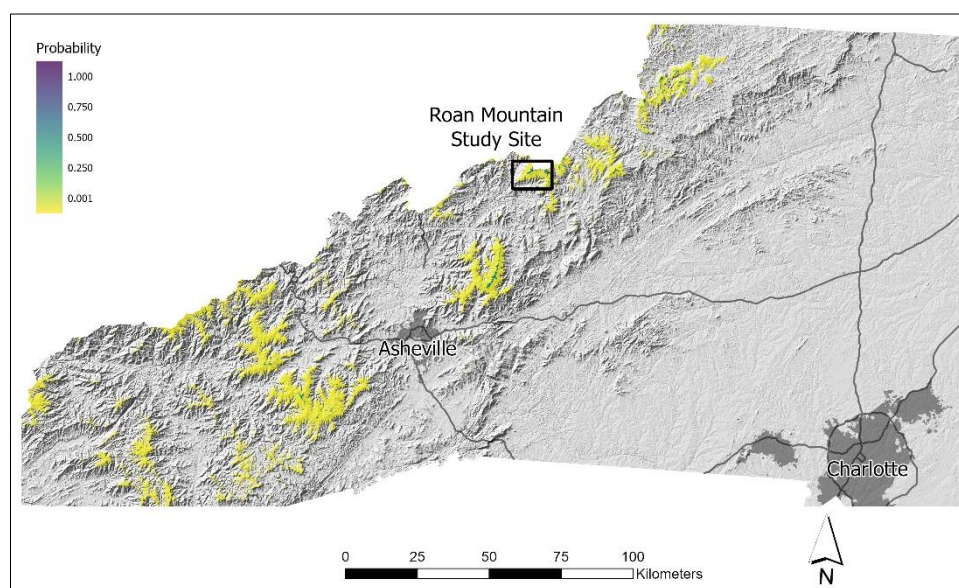
Figure 10. Maxent probability raster for the entire Blue Ridge region. Because of the rareness of the habitat, the high probability areas are hard to differentiate at this scale. Darker colors indicate higher probability areas that are suitable for *Geum radiatum*.

The Maxent summary output suggested elevation, soils, and distance from water were the most important variables overall, contributing to 90% of the model solution (see Appendix A, Table A1). Elevation represented the most critical predictor in explaining species distribution for *Geum radiatum*. Analysis of the response curves indicated elevations over 1800 m, Balsam sandy loam and Wayah–Burton complex soils, increasing distance from hydrographic features, high solar insolation values, and north-northwest aspects are the most important attributes within each predictor (see Appendix A, Figure A3).

3.2. Targeted Flight Plan and UAS Data

Isolines generated from the predictive model for the 230,955 km^2 Blue Ridge ecoregion resulted in 173 polygons totaling 1840 km^2 with a 95% probability that environmental conditions are suitable for *Geum radiatum* (Figure 11). The high probability polygons were in high-elevation areas with bare cliffs and forested areas in steep terrain.
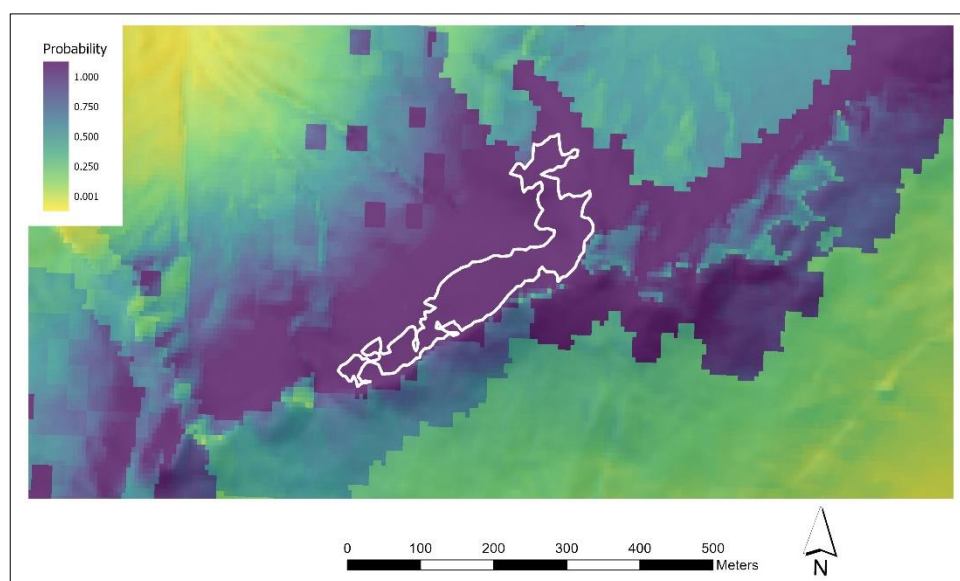
Figure 11. A subregion of the entire modeled Blue Ridge region zoomed to the Roan Mountain study site. Darker colors indicate higher probability areas that are suitable for *Geum radiatum*. The white line used for the flight plan represents an area with at least 95% probability that environmental conditions are suitable for *Geum radiatum*.

Three flights executed at the selected site at Roan Mountain included the 95% probability polygon with an overall flight time of 53 min. A total of 814 photos were collected, 596 on the first flight, 145 on the second, and 73 on the third. An orthomosaic with 1.67 cm/px ground resolution was generated from the combined nadir aerials and oblique cliff photography. The resolution of the DSM was 3.54 cm per pixel, and the colorized point cloud contained 232 million points at a density of 2605 ppm^2. These resolutions provided a high level of detail, more than sufficient for visual identification of the unique *Geum radiatum* leaf shape, color, and bright yellow blooms, where a single rosette measures around 6.5 cm^2 and a patch of rosettes can cover 1.7 m^2 [23].

3.3. Analysis of Geum Radiatum Locations

3.3.1. Results of Visual Analysis

The location of 33 known plants was verified by visual analysis of acquired UAS images, and coordinates of their reference points were digitized on the georeferenced orthomosaic. This allowed us to record locations of individual plants at much higher accuracy than the previously known, approximate NHP polygon.

Four new plants were discovered within the 95% probability flight area. Three were located on the cliff face just outside of the NHP polygons. One, especially large plant, was found within an atypical, forested area (Figures 12 and 13). Although this plant is within a NHP polygon area, it was previously undocumented. Additionally, a flowering plant in a shaded canopy gap was identified as a potential *Geum radiatum* but remained a probable location to investigate (Figures 12 and 14).
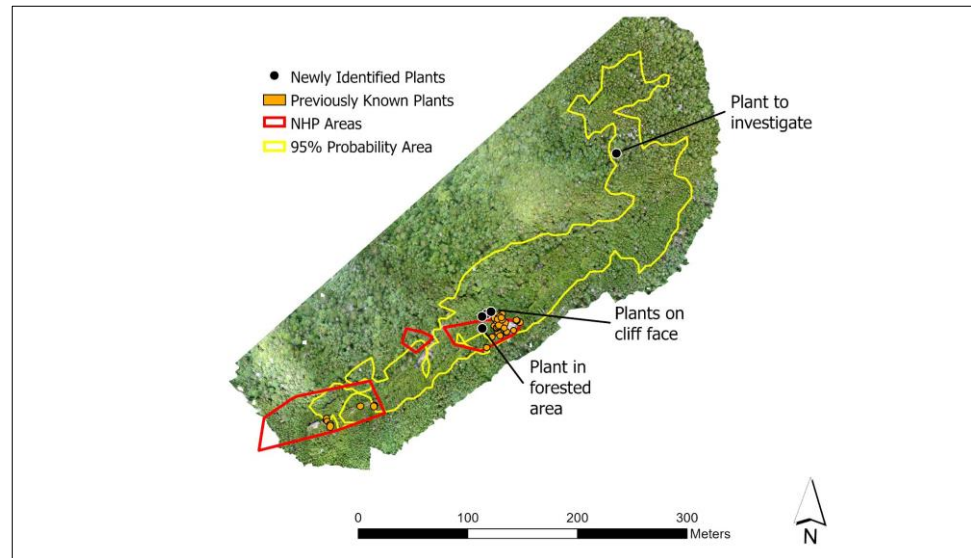
Figure 12. Previously known and newly identified *Geum radiatum* plant locations digitized from orthomosaic. Of the newly discovered plants, three plants were found on the cliff face, one was found in the canopy gap, and one probable plant location to investigate. Locations of the previously known plants within the polygons were recorded, and new plants were identified.

Figure 13. One previously unknown location of *Geum radiatum* in a forested area. Nadir aerial photo from UAS (**a**); and oblique aerial photo (**b**).
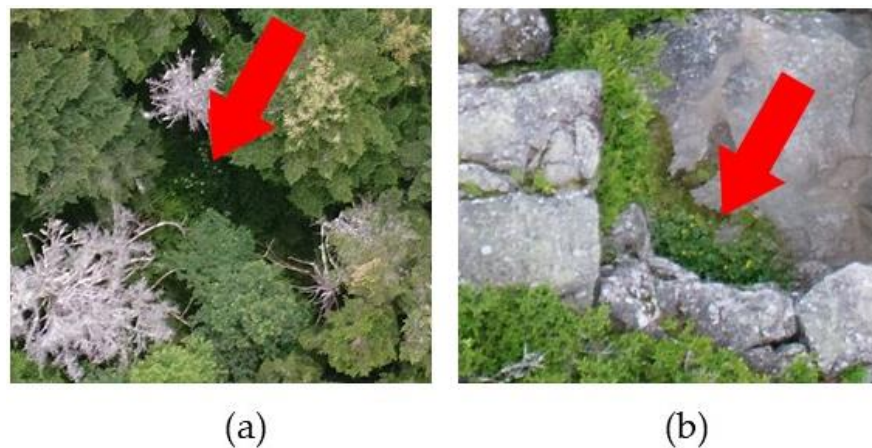
Figure 14. Possible location of flowering *Geum radiatum* plant (**a**); documented *Geum radiatum* location for comparison (**b**).

3.3.2. Computer Vision

First, *Geum radiatum* photos were acquired with the UAS camera for testing purposes as it was being held by hand. The YOLOv3 object detection program, trained for *Geum radiatum,* was able to identify the plant in these photos, even among other leaves, and with varying light conditions (Figure 15).

Figure 15. Results from the YOLOv3 model for two photos acquired by UAS camera on the ground with *Geum radiatum* shown by green object detection boxes, including the confidence level of the detection.

However, it was impossible to detect and identify *Geum radiatum* plants in any of the 814 nadir and oblique UAS photos collected in the project using the object detection program. Images taken at the ground level had leaf diameters captured by approximately 300 pixels (Figure 2). In contrast, the aerial images had leaf diameters represented by approximately 10 pixels (Figure 14) which were insufficient to capture the leaf shape with the detail needed for automated detection.

4. Discussion

This research highlights the use of machine learning to plan targeted UAS flights for rare plant monitoring, demonstrated by a case study mapping *Geum radiatum* in the Blue Ridge Mountains ecoregion. To our knowledge, this is the first study that has used a species distribution model to create targeted UAS flight areas to map locations of rare and endangered plant species. Targeting the UAS flights is important because the overcollection of data over broad areas increases battery power consumption. Battery capacity and discharge rate are the primary factors affecting the duration of UAS missions. Having multiple batteries at hand or flying at higher altitudes to capture more area per image are not ideal solutions because batteries are heavy to transport to remote field sites, and flying at higher altitudes would decrease the detail of the imagery such that the mapped plant might not be identified. Additionally, targeted flight areas allow for faster data collection so that changing weather and lighting conditions do not affect the final imagery products [6].

Species distribution modeling using Maxent identified high probability areas with suitable conditions for *Geum radiatum* with a high level of certainty. Still, the 95% probability polygon included non-bluff areas where *Geum radiatum* is not typically found. Investigating the variable contributions to the model shows that soils and elevation had the most influence on the result. However, these two predictors are not directly associated with bluff areas. Although the 95% probability polygon contains unlikely habitat for the plant, there was one probable plant location to investigate in the atypical area. Additional environmental variables, such as geology, landforms, and vegetation structure from LiDAR [71] or UAS orthomosaic [72], could improve the Maxent results. For example, one confirmed *Geum radiatum* plant and another possible plant are in gaps in the forest canopy. Canopy

gaps allow enough light for plant survival as well as for identification in UAS imagery. Multiple points from within the NHP polygons or precise *Geum radiatum* locations mapped from the orthomosaic can be used as training data to improve flight planning over time and potentially discover previously unknown individuals.

The selection of the probability threshold used to derive flight area depends on the goal of the mapping and available resources. It is possible plants might be located at lower probability thresholds outside of the 95% probability boundary used in this study. Moreover, to further validate the predictive model results, it would be useful to fly zero to very low probability areas to confirm that both conditions for presence and absence of the modeled species are adequately represented by the model.

Preparing environmental data for Maxent data can introduce uncertainties from resampling that need to be handled appropriately. Five of the six most important variables contributing to the model were derived from the 6 m elevation dataset, and no resampling was necessary. The coarser resolution data, such as landcover, was not an influencing factor at the 30 m resolution indicating that the resolution of this dataset was too low to play a role in the predictive modeling or the landcover indeed does not influence the distribution of the studied plant species. The impact of the landcover variable could be different and potentially further improve the modeling results if this layer were derived from higher resolution data such as 1 m resolution National Agriculture Imagery Program (NAIP) or UAS orthomosaics. However, we believe that the modeling results were more than adequate for flight planning, where our focus was on outlining a mapping area rather than the precise location of the plants.

Although the object detection approach successfully detected plants in on-ground images, it was not possible to identify occurrences of Geum radiatum from UAS collected imagery. The model failed because it was trained with plant images captured at close range or ground level, with resolutions approximately 30 times greater than the aerial UAS imagery. We anticipate that object detection performance will improve with training using UAS imagery collected at similar distances and angles [69] or with different, higher-resolution, or multispectral sensors. Future work is planned to label and train an object detection model using UAS imagery and plant locations collected during this project to analyze the images taken in subsequent flights. In addition, we will collect images under varying environmental conditions and at specific heights to determine the threshold at which the plant cannot be detected anymore. Finally, experimentation with an object detection method UAS-YOLO, specifically designed to detect small objects in UAS imagery [69], is underway.

Ground control points (GCPs) and checkpoints are important for processing drone imagery and estimating accuracy. We brought global navigation satellite system (GNSS) survey equipment and aerial targets to Roan Mountain on flight days, but the extreme relief and heavy tree cover made placement of GCPs impractical. Positional information from the onboard UAS GNSS receivers was used in processing with sufficient results. The only photo identifiable feature in the ortho imagery is the platform used for flight operations. Width measurements between the platform in the UAS orthomosaic and NC OneMap imagery [73] were within 3 cm of each other. Measurements from the platform corners showed a horizontal accuracy under 1.5 m. A real-time kinematic (RTK) or post-processed kinematic (PPK) capable UAS can mitigate positional accuracy problems. However, these types of UAS are not a substitute for checkpoints to verify the accuracy of final products. In areas where it is challenging to perform survey work, conservation organizations will have to balance the benefits of positional accuracy with the cost of RTK UAS equipment and GCP survey.

We selected ten environmental parameters (map layers) in the Blue Ridge region that were relevant predictors of Geum radiatum habitat, although a total of 16 environmental layers were created for the entire state of North Carolina as part of this work. The relevant layers can be selected based on applicability to the species of interest. This will allow us to scale to a larger region by applying a similar methodology to other rare or endangered

plant species in the state. Current conservation practices can be transformed by prioritizing monitoring areas using the continuously improving probability maps and tracking the status of the monitored plants over time. Additionally, the monitored areas can be extended as the process becomes more automated and the state of the entire ecosystem supporting the rare plants can be assessed. The regional adaptation of the proposed approach would require us to equip regional managers and their personnel with multiple drones, which is facilitated by focusing on low-cost equipment. At the same time, the Maxent modeling and the environmental variables can be provided as an online application. We are working on a project similar to the one presented in this paper to identify Virginia spiraea with UAS along waterways in the mountains of North Carolina to assist an electric utility with regulatory compliance.

5. Conclusions

This research provides a data-driven approach to plan flight areas from predictive modeling, which will improve UAS data collection and processing efficiencies. Using a machine-learning predictive model, we created targeted flight plans to collect data in areas with a high probability of a target plant. This technique reduces battery requirements and data storage needs as well as flight and processing time. The model also offers insight into which variables were significant in determining the monitored plant, *Geum radiatum*, distribution. The UAS imagery was sufficient to identify the plants' locations and discover four previously unknown *Geum radiatum* occurrences. Of the five actions listed in the USFWS recovery plan for *Geum radiatum*, this research has the potential to contribute to two; (1) the survey of suitable habitat for additional populations and (2) monitor and protect existing populations. Finally, the 2020 USFWS 5-year review for *Geum radiatum* recommends the agency continue working with and supporting efforts to identify rare species using UAS [28] (p. 31). This study demonstrates that UAS and machine learning can enhance future monitoring efforts for additional rare or endangered plants.

Appendix A

Figure A1. Average omission and predicted area for *Geum radiatum*. Test omission rate and predicted area averaged over the replicate runs.
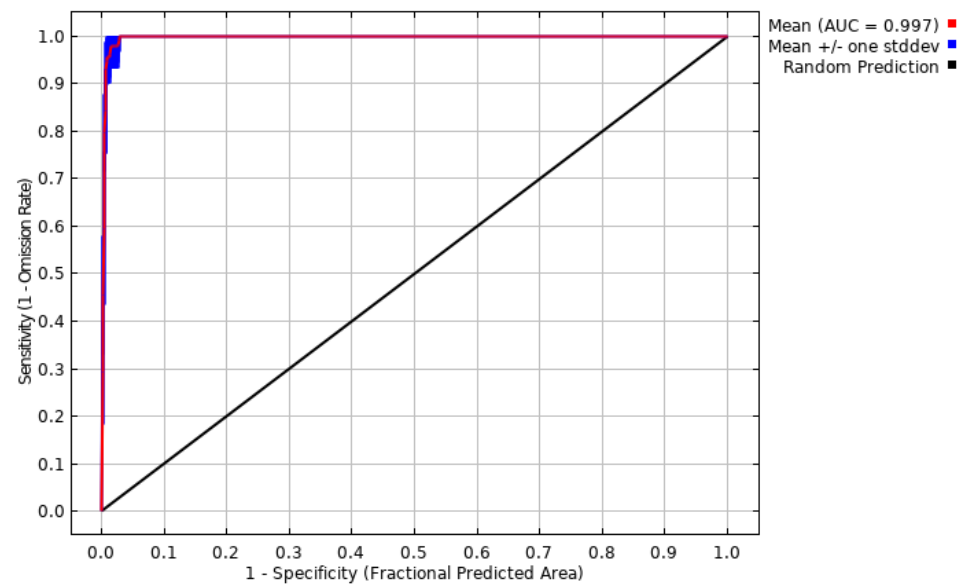
Figure A2. Average sensitivity vs. (1—specificity) for *Geum radiatum* and receiver operating characteristic (ROC) curve averaged over the replicate runs.

Table A1. Estimates of relative contributions of the most important environmental variables in the Maxent model for *Geum radiatum*.

Variable	elevation	soils	dist. to water	solar	aspect	slope
Contribution [%}	70.1	16.8	5.3	2.7	1.9	1.0
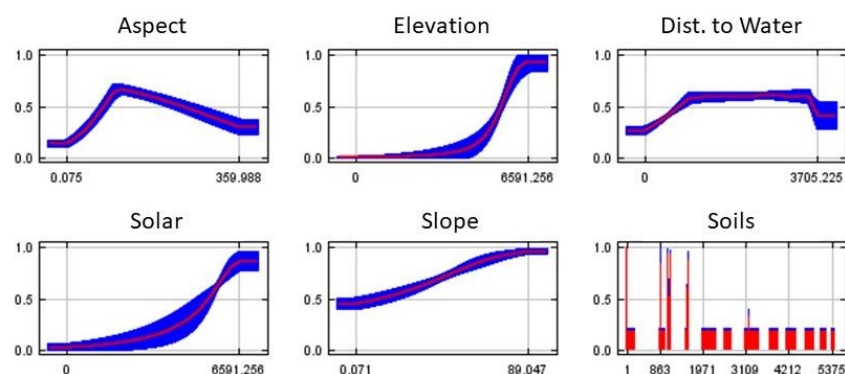
Figure A3. Maxent response curves of the most important variables displaying the mean response of the five replicate Maxent runs (red) and the mean $+/-$ one standard deviation (blue). The response curves with bars are for categorical variables, and the lines are for continuous variables. The categorical variable numbers respond to classes in the dataset.

References

1. Alexander, H.M.; Reed, A.W.; Kettle, W.D.; Slade, N.A.; Roels, S.A.B.; Collins, C.D.; Salisbury, V. Detection and Plant Monitoring Programs: Lessons from an Intensive Survey of Asclepias meadii with Five Observers. *PLoS ONE* **2012**, *7*, e52762. [CrossRef]
2. Elzinga, C.L.; Salzer, D.W.; Willoughby, J.W. *Nature Conservancy (U.S.) Measuring & Monitoring Plant Populations; U.S. Dept. of the Interior, Bureau of Land Management*; Nature Conservancy: Arlington, VA, USA, 1998; Volume 1730-1.
3. North Carolina General Assembly Endangered and Threatened Wildlife and Wildlife Species of Special Concern. 1979. Available online: https://www.ncleg.net/EnactedLegislation/Statutes/HTML/ByArticle/Chapter_113/Article_25.html (accessed on 15 January 2020).
4. Strumia, S.; Buonanno, M.; Aronne, G.; Santo, A.; Santangelo, A. Monitoring of Plant Species and Communities on Coastal Cliffs: Is the Use of Unmanned Aerial Vehicles Suitable? *Diversity* **2020**, *12*, 149. [CrossRef]
5. Rominger, K.; Meyer, S.E. Application of UAV-Based Methodology for Census of an Endangered Plant Species in a Fragile Habitat. *Remote Sens.* **2019**, *11*, 719. [CrossRef]
6. Jaud, M.; Letortu, P.; Théry, C.; Grandjean, P.; Costa, S.; Maquaire, O.; Davidson, R.; Le Dantec, N. UAV survey of a coastal cliff face–Selection of the best imaging angle. *Meas. J. Int. Meas. Confed.* **2019**, *139*, 10–20. [CrossRef]
7. Groos, A.R.; Bertschinger, T.J.; Kummer, C.M.; Erlwein, S.; Munz, L.; Philipp, A. The Potential of Low-Cost UAVs and Open-Source Photogrammetry Software for High-Resolution Monitoring of Alpine Glaciers: A Case Study from the Kanderfirn (Swiss Alps). *Geoscience* **2019**, *9*, 356. [CrossRef]
8. Rossini, M.; Di Mauro, B.; Garzonio, R.; Baccolo, G.; Cavallini, G.; Mattavelli, M.; De Amicis, M.; Colombo, R. Rapid melting dynamics of an alpine glacier with repeated UAV photogrammetry. *Geomorphology* **2018**, *304*, 159–172. [CrossRef]
9. Šašak, J.; Gallay, M.; Kaňuk, J.; Hofierka, J.; Minár, J. Combined Use of Terrestrial Laser Scanning and UAV Photogrammetry in Mapping Alpine Terrain. *Remote Sens.* **2019**, *11*, 2154. [CrossRef]
10. Vivero, S.; Lambiel, C. Monitoring the crisis of a rock glacier with repeated UAV surveys. *Geogr. Helv.* **2019**, *74*, 59–69. [CrossRef]
11. López, J.J.; Mulero-Pázmány, M. Drones for Conservation in Protected Areas: Present and Future. *Drones* **2019**, *3*, 10. [CrossRef]
12. Shaffer, M.J.; Bishop, J.A. Predicting and Preventing Elephant Poaching Incidents through Statistical Analysis, GIS-Based Risk Analysis, and Aerial Surveillance Flight Path Modeling. *Trop. Conserv. Sci.* **2016**, *9*, 525–548. [CrossRef]
13. Tu, Y.-H.; Phinn, S.; Johansen, K.; Robson, A.; Wu, D. Optimising drone flight planning for measuring horticultural tree crop structure. *ISPRS J. Photogramm. Remote Sens.* **2020**, *160*, 83–96. [CrossRef]
14. Lin, L.; Goodrich, M.A. UAV intelligent path planning for Wilderness Search and Rescue. In Proceedings of the 2009 IEEE/RSJ International Conference on Intelligent Robots and Systems, St. Louis, MO, USA, 11–15 October 2009; pp. 709–714.
15. Pérez-Carabaza, S.; Scherer, J.; Rinner, B.; López-Orozco, J.A.; Besada-Portas, E. UAV trajectory optimization for Minimum Time Search with communication constraints and collision avoidance. *Eng. Appl. Artif. Intell.* **2019**, *85*, 357–371. [CrossRef]
16. Juan, V.S.; Santos, M.; Andújar-Márquez, J.M. Intelligent UAV Map Generation and Discrete Path Planning for Search and Rescue Operations. *Complexity* **2018**, *2018*, 1–17. [CrossRef]
17. Fitzpatrick, M.; Reis, G.M.; Anderson, J.; Bobadilla, L.; Al Sabban, W.; Smith, R.N. Development of environmental niche models for use in underwater vehicle navigation. *IET Cyber-Syst. Robot.* **2020**, *2*, 67–77. [CrossRef]
18. Phillips, S.J.; Anderson, R.P.; Schapire, R.E. Maximum entropy modeling of species geographic distributions. *Ecol. Model.* **2006**, *190*, 231–259. [CrossRef]
19. US Fish and Wildlife Service Spreading Avens (Geum Radiatum) Recovery Plan. 1993. Available online: http://ecos.fws.gov/docs/recovery_plans/1993/930428.pdf (accessed on 11 March 2018).
20. Massey, J.; Atkinson, T.; Whitson, P. *Endangered and Threatened Plant Survey of 12 Species in the Eastern Part of Region IV*; 1980; USFWS Contract 14-160004-78-108. Report. Available online: https://ecos.fws.gov/ecp/report/table/critical-habitat.html (accessed on 20 June 2020).

21. Massey, J.R. *An Atlas and Illustrated Guide to the Threatened and Endangered Vascular Plants of the Mountains of North Carolina and Virginia*; Southeastern Forest Experiment Station: Asheville, NC, USA, 1983; Volume 20.

22. US Fish and Wildlife Service Spreading Avens Fact Sheet. 2011. Available online: https://www.fws.gov/asheville/pdfs/SpreadingAvens_factsheet.pdf/ (accessed on 15 January 2018).

23. Peeples, G. Botanists Blitz Area Cliffs for Endangered Plant. 2008. Available online: https://www.fws.gov/southeast/articles/botanists-blitz-area-cliffs-for-endangered-plant/ (accessed on 19 May 2020).

24. Godt, M.J.W.; Johnson, B.R.; Hamrick, J. Genetic Diversity and Population Size in Four Rare Southern Appalachian Plant Species. *Conserv. Biol.* **1996**, *10*, 796–805. [CrossRef]

25. Schafale, M.P.; Weakley, A.S. *North Carolina Natural Heritage Program Classification of the Natural Communities of North Carolina: Third Approximation; North Carolina Natural Heritage Program, Division of Parks and Recreation*; Department of Environment, Health, and Natural Resources: Raleigh, NC, USA, 1990.

26. Harrison, S.; Noss, R. Endemism hotspots are linked to stable climatic refugia. *Ann. Bot.* **2017**, *119*, 207–214. [CrossRef]

27. Pittillo, J.D.; Hatcher, R.D.; Buol, S.W. Introduction to the Environment and Vegetation of the Southern Blue Ridge Province. *Castanea* **1998**, *63*, 202–216.

28. US Fish and Wildlife Service Spreading Avens (Geum Radiatum) 5-Year Review: Summary and Evaluation. 2020. Available online: https://ecos.fws.gov/docs/tess/species_nonpublish/2953.pdf/ (accessed on 20 June 2020).

29. Ulrey, C.; Quintana-Ascencio, P.F.; Kauffman, G.; Smith, A.; Menges, E.S. Life at the top: Long-term demography, microclimatic refugia, and responses to climate change for a high-elevation southern Appalachian endemic plant. *Biol. Conserv.* **2016**, *200*, 80–92. [CrossRef]

30. Maxent Software for Modeling Species Niches and Distributions, Version 3.4.1. Available online: http://biodiversityinformatics.amnh.org/open_source/maxent (accessed on 15 March 2018).

31. Phillips, S.J.; Anderson, R.P.; Dudík, M.; Schapire, R.E.; Blair, M.E. Opening the black box: An open-source release of Maxent. *Ecography* **2017**, *40*, 887–893. [CrossRef]

32. Wiser, S.K.; Peet, R.K.; White, P.S. Prediction of Rare-Plant Occurrence: A Southern Appalachian Example. *Ecol. Appl.* **1998**, *8*, 909. [CrossRef]

33. Gobeyn, S.; Mouton, A.M.; Cord, A.F.; Kaim, A.; Volk, M.; Goethals, P.L. Evolutionary algorithms for species distribution modelling: A review in the context of machine learning. *Ecol. Model.* **2019**, *392*, 179–195. [CrossRef]

34. Hijmans, R.J.; Elith, J. Species Distribution Modeling with R.R CRAN Project. 2013. Available online: https://citeseerx.ist.psu.edu/viewdoc/download?doi=10.1.1.190.9177&rep=rep1&type=pdf/ (accessed on 23 September 2019).

35. Elith, J.; Graham, C.H.; Anderson, R.P.; Dudík, M.; Ferrier, S.; Guisan, A.; Hijmans, R.J.; Huettmann, F.; Leathwick, J.R.; Lehmann, A.; et al. Novel methods improve prediction of species' distributions from occurrence data. *Ecography* **2006**, *29*, 129–151. [CrossRef]

36. Elith, J.; Phillips, S.J.; Hastie, T.; Dudík, M.; Chee, Y.E.; Yates, C.J. A statistical explanation of MaxEnt for ecologists. *Divers. Distrib.* **2011**, *17*, 43–57. [CrossRef]

37. Helliwell, R.; Chapman, J. Use of Species Distribution Models in Conservation Biology. Report on File with Interagency Special Status/Sensitive Species Program. 2013. Available online: https://www.fs.fed.us/r6/sfpnw/issssp/documents4/inv-rpt-use-of-species-dist-models-in-cons-bio-201302.pdf/ (accessed on 15 March 2018).

38. Merow, C.; Smith, M.J.; Silander, J.A. A practical guide to MaxEnt for modeling species' distributions: What it does, and why inputs and settings matter. *Ecography* **2013**, *36*, 1058–1069. [CrossRef]

39. North Carolina Natural Heritage Program. Natural Heritage Element Occurrences. Available online: https://ncnhde.natureserve.org/content/data-download (accessed on 28 June 2018).

40. QGIS Development Team. QGIS Geographic Information System. Open Source Geospatial Foundation Project. 2019. Available online: http://qgis.osgeo.org (accessed on 22 November 2016).

41. North Carolina Floodplain Mapping Program. North Carolina 20 Ft DEM. Available online: http://geodata.lib.ncsu.edu/NCElev (accessed on 19 March 2018).

42. Suri, M.; Hofierka, J. A New GIS-based Solar Radiation Model and Its Application to Photovoltaic Assessments. *Trans. GIS* **2004**, *8*, 175–190. [CrossRef]

43. U.S. Geological Survey. North Carolina National Land Cover Data Set (NLCD). Available online: https://nrcs.app.box.com/v/gateway/folder/22222601427 (accessed on 5 March 2018).

44. U.S. Geological Survey (USGS). Gap Analysis Project (GAP), 2016, GAP/LANDFIRE National Terrestrial Ecosystems 2011: U.S. Geological Survey data release. [CrossRef]

45. Soil Survey Staff. The Gridded Soil Survey Geographic (SSURGO) Database for North Carolina. Available online: https://gdg.sc.egov.usda.gov/ (accessed on 7 March 2018).

46. U.S. Geological Survey. National Hydrography Dataset (NHD). U.S. Geological Survey. 2017. Available online: http://nhd.usgs.gov/ (accessed on 10 June 2017).

47. North Carolina Department of Transportation. Statewide System & Non-System Road Routes. Available online: https://connect.ncdot.gov/resources/gis/pages/gis-data-layers.aspx (accessed on 26 March 2018).

48. GRASS GIS. Available online: https://grass.osgeo.org/ (accessed on 25 March 2021).

49. U.S. Environmental Protection Agency. Level III and IV Ecoregions of the Continental United States. Available online: https://www.epa.gov/eco-research/level-iii-and-iv-ecoregions-continental-united-states (accessed on 19 March 2018).

50. Young, N.; Carter, L.; Evangelista, P. A MaxEnt Model v3. 3.3 e Tutorial (ArcGIS V10). Natural Resource Ecology Laboratory, Colorado State University and the National Institute of Invasive Species Science. 2011. Available online: https://ibis.colostate.edu/webcontent/ws/coloradoview/tutorialsdownloads/a_maxent_model_v7.pdf(accessed on 30 June 2020).

51. Phillips, S.J.; Dudík, M. Modeling of species distributions with Maxent: New extensions and a comprehensive evaluation. *Ecography* **2008**, *31*, 161–175. [CrossRef]

52. Phillips, S.J. A Brief Tutorial on Maxent. 2017. Available online: http://biodiversityinformatics.amnh.org/open_source/maxent/ (accessed on 3 January 2019).

53. U.S. Geological Survey. 1:24,000 Topo Map. Bakersville, NC. 1997. Available online: https://ngmdb.usgs.gov/topoview (accessed on 11 October 2018).

54. Brown, D.M. Vegetation of Roan Mountain: A Phytosociological and Successional Study. *Ecol. Monogr.* **1941**, *11*, 61–97. [CrossRef]

55. DroneDeploy Web App. Available online: https://www.dronedeploy.com/ (accessed on 3 January 2018).

56. DroneDeploy User Documentation. V.3. Available online: https://support.dronedeploy.com/docs (accessed on 22 March 2018).

57. Bonnet, S.; Lisein, J.; Lejeune, P. Comparison of UAS photogrammetric products for tree detection and characterization of coniferous stands. *Int. J. Remote Sens.* **2017**, *38*, 5310–5337. [CrossRef]

58. NC Floodplain Mapping Program. Digital Elevation Model, DEM03. Available online: https://sdd.nc.gov/ (accessed on 14 March 2018).

59. DroneDeploy Flight App. V.2.73.0. Available online: https://www.dronedeploy.com (accessed on 10 June 2018).

60. DJI GO. V.4.2.14. Available online: https://www.dji.com/goapp (accessed on 23 May 2018).

61. Agisoft PhotoScan Software. Agisoft Metashape. Available online: https://www.agisoft.com/ (accessed on 30 January 2020).

62. Agisoft Metashape User Manual Version 1.5. 2019. Available online: https://www.agisoft.com/pdf/metashape-pro_1_5_en.pdf (accessed on 30 January 2020).

63. Jayathunga, S.; Owari, T.; Tsuyuki, S. Evaluating the Performance of Photogrammetric Products Using Fixed-Wing UAV Imagery over a Mixed Conifer–Broadleaf Forest: Comparison with Airborne Laser Scanning. *Remote Sens.* **2018**, *10*, 187. [CrossRef]

64. ImportPhotos: A QGIS Plugin to Visualise Geotagged Photos. v.2.2. Available online: https://mariosmsk.com/2019/07/02/qgis-plugin-importphotos/ (accessed on 16 July 2019).

65. Zheng, C.; Abd-Elrahman, A.; Whitaker, V. Remote Sensing and Machine Learning in Crop Phenotyping and Management, with an Emphasis on Applications in Strawberry Farming. *Remote Sens.* **2021**, *13*, 531. [CrossRef]

66. Microsoft/VOTT: Visual Object Tagging Tool. Available online: https://github.com/microsoft/VoTT (accessed on 22 April 2018).

67. Darknet: Open Source Neural Networks in C. Available online: http://pjreddie.com/darknet (accessed on 11 February 2020).

68. Dorrer, M.; Popov, A.A.; Tolmacheva, A.E. Building an artificial vision system of an agricultural robot based on the DarkNet system. *IOP Conf. Ser. Earth Environ. Sci.* **2020**, *548*, 032032. [CrossRef]

69. Liu, M.; Wang, X.; Zhou, A.; Fu, X.; Ma, Y.; Piao, C. UAV-YOLO: Small Object Detection on Unmanned Aerial Vehicle Perspective. *Sensors* **2020**, *20*, 2238. [CrossRef]

70. Redmon, J.; Farhadi, A. YOLOv3: An Incremental Improvement. 2018. Available online: https://pjreddie.com/yolo/ (accessed on 20 April 2019).

71. Petras, V.; Newcomb, D.J.; Mitasova, H. Generalized 3D fragmentation index derived from lidar point clouds. *Open Geospat. Data Softw. Stand.* **2017**, *2*, 19. [CrossRef]

72. Bagaram, M.B.; Giuliarelli, D.; Chirici, G.; Giannetti, F.; Barbati, A. UAV Remote Sensing for Biodiversity Monitoring: Are Forest Canopy Gaps Good Covariates? *Remote Sens.* **2018**, *10*, 1397. [CrossRef]

73. North Carolina OneMap. Latest Orthoimagery. Available online: https://services.nconemap.gov/secure/rest/services/Imagery/Orthoimagery_Latest/ImageServer (accessed on 19 January 2020).